Co-ordination Chemistry of Mixed Pyridine–Phenol Ligands; Electrochemical, Electron Paramagnetic Resonance and Structural Studies on Mononuclear Ruthenium(III) and Chromium(III) Complexes†

David A. Bardwell, Daniel Black, John C. Jeffery, Erik Schatz and Michael D. Ward*
School of Chemistry, University of Bristol, Cantock's Close, Bristol BS8 1TS, UK

Syntheses of the new complexes $[RuL^1_3]$ **1**, $[RuL^1_2(acac)]$ **2**, $[RuL^1_2(bipy)][PF_6]$ **3**, $[CrL^1_3]$ **4**, $[CrL^1_2(acac)]$ **5** and $[CrL^2_2][PF_6]$ **6** [HL^1 = 2-(2-hydroxyphenyl)pyridine, HL^2 = 6-(2-hydroxyphenyl)-2,2'-bipyridine, Hacac = pentane-2,4-dione, bipy = 2,2'-bipyridine] have been carried out. The ruthenium(III) complexes **1**–**3** all show reversible +3/+4 and +2/+3 waves in their cyclic voltammograms. Together with some previously reported complexes, a full set of electrochemical data is now available for ruthenium complexes with donor sets varying from N_6 to N_3O_3 (where N denotes a pyridyl donor and O a phenolate donor); there is a monotonic decrease of 0.75 V in the Ru^{II}–Ru^{III} couple per additional phenolate in the co-ordination sphere. Both **1** and **2** have typical rhombic EPR spectra, but the spectrum of **3** is only consistent with formation of a mixture of *cis* and *trans* isomers. The chromium(III) complexes show similar variations in the potentials of their metal-centred reductions with donor set although the relationship is not linear. X-Ray analysis showed that both **4** and **6** have pseudo-octahedral crystal structures. Complex **4** crystallises in the chiral space group *Fdd*2 and therefore spontaneously resolves on crystallisation; **6** has a π-stacking interaction between aromatic residues of adjacent complex units, with an average separation of 3.71 Å between the atoms of one aromatic ring and the mean plane of the other.

We have recently been interested in the co-ordination chemistry of polydentate chelating ligands which contain mixed pyridine–phenol and phenanthroline–phenol donor sets.[1–5] The resulting complexes have proved to be interesting for a variety of reasons. Some unusual structures for copper(II) and nickel(II) complexes have been established in which non-covalent interactions such as hydrogen bonding and π stacking appear to play a dominant part;[1–3] the binuclear phenolate-bridged copper(II) complexes are antiferromagnetically coupled with exceptionally well resolved triplet EPR spectra,[4] and, by varying the numbers of pyridyl and phenolate ligands in metal-ion co-ordination spheres, the redox potentials of the complexes may be varied over a wide range.[1,5]

In this paper we describe the preparation, and electrochemical and spectroscopic properties of a series of binary and ternary complexes of ruthenium(III) and chromium(III) using the ligands 2-(2-hydroxyphenyl)pyridine (HL^1) and 6-(2-hydroxyphenyl)-2,2'-bipyridine (HL^2). The study of the redox and spectroscopic properties of pseudo-octahedral complexes of ruthenium(III) with bidentate N,O-donor ligands such as salicylaldimines and 8-hydroxyquinoline has attracted considerable attention recently,[6–8] and our ligand HL^1 (containing phenolic oxygen and sp^2-hybridised nitrogen donors) permits an extension of this work. Chromium(III) complexes of this type are, in contrast, much rarer.[8,9]

Experimental

Fast-atom bombardment (FAB) mass spectra were recorded on a VG-Autospec instrument at the SERC Mass Spectrometry Service Centre, Swansea. Electronic spectra were recorded on Perkin Elmer Lambda 2 or Lambda 19 spectrophotometers, in CH_2Cl_2 (UV/VIS region) or CCl_4 (near-IR region) solutions. The EPR spectra were recorded as frozen glasses in CH_2Cl_2–thf mixtures at 77 K on a Bruker ESP-300E spectrometer. Electrochemical experiments were performed using an EG&G PAR model 273A potentiostat. A standard three-electrode configuration was used, with platinum-bead working and auxiliary electrodes and a saturated calomel electrode (SCE) reference. Ferrocene was added at the end of each experiment as an internal standard; all potentials are quoted *vs.* the ferrocene–ferrocenium couple. The solvent was acetonitrile, purified by distillation twice from CaH_2, with 0.1 mol dm^{-3} $[NBu_4][PF_6]$ as base electrolyte. All solvents were dried by standard methods before use. The ligands HL^1 (ref. 5) and HL^2 (ref. 1) were prepared as described previously. The compounds $[Ru(bipy)Cl_3]$ (bipy = 2,2'-bipyridine)[10] and $[Ru(acac)_3]$ [Hacac = acetylacetone(pentane-2,4-dione)][11] were prepared according to published methods. All starting materials were obtained from Aldrich and used as received.

Preparations.—$[RuL^1_3]$ **1** *and* $[RuL^1_2(acac)]$ **2**. A mixture of $[Ru(acac)_3]$ (0.3 g, 0.75 mmol) and HL^1 (0.43 g, 2.5 mmol) in ethylene glycol (15 cm^3) was heated to 175 °C for 3 h, whilst bubbling a slow stream of nitrogen through the mixture (approximately 1 bubble per second). After cooling to room temperature, the mixture was diluted with water (70 cm^3) and extracted with CH_2Cl_2 (4 × 15 cm^3). The combined organic extracts were dried ($MgSO_4$) and then chromatographed on alumina (Brockmann activity III) with CH_2Cl_2 as eluent. The initial small red-purple band was collected and evaporated to dryness to give the minor product $[RuL^1_2(acac)]$ (0.037 g, 9%). The major red-brown fraction was then collected and evaporated to dryness to give pure $[RuL^1_3]$ (0.41 g, 90%). Both complexes were recrystallised from acetonitrile–diethyl ether.

$[Ru(bipy)L^1_2][PF_6]$ **3**. A mixture of $[Ru(bipy)Cl_3]$ (0.182 g, 0.5 mmol) and acetylacetone (1 cm^3, excess) was heated to reflux in EtOH–water (15 cm^3, 3:1 v/v) for 3.5 h and then

† *Supplementary data available:* see Instructions for Authors, *J. Chem. Soc., Dalton Trans.*, 1993, Issue 1, pp. xxiii–xxviii.

evaporated to dryness *in vacuo*. The dark red [Ru(bipy)-(acac)$_2$]Cl was redissolved in ethylene glycol (15 cm^3), and HL^1 (0.188 g, 1.1 mmol) added. The mixture was then heated to 175 °C for 1.5 h with N_2 bubbling through it slowly (as for **1**, above); after about 15 min the colour had changed from deep red to dark green. After allowing the reaction to cool, water (100 cm^3) was added to give a dark solution, from which a dark green solid was precipitated on addition of NH_4PF_6. The solid was filtered off, washed with water, allowed to dry in air, and chromatographed on alumina (Brockmann activity III) with CH_2Cl_2 as eluent. The major blue-green band was collected and evaporated to dryness to give pure [Ru(bipy)L$^1{}_2$][PF$_6$] (0.24 g, 64%), which was recrystallised from acetonitrile–diethyl ether to give small dark green blocks.

[CrL$^1{}_3$] **4**. *Method A*. A mixture of $CrCl_3 \cdot 6H_2O$ (0.133 g, 0.5 mmol), HL^1 (0.257 g, 1.5 mmol) and Na_2CO_3 (0.16 g, 1.5 mmol) was heated to reflux in ethanol (15 cm^3) for 3 h, during which time a dark precipitate appeared. After allowing the reaction to cool to room temperature and adding water (15 cm^3), the precipitate was collected by filtration, dried in air, and chromatographed on alumina (Brockmann activity III) with CH_2Cl_2 as eluent. The major red-green band was collected and evaporated to dryness to give pure [CrL$^1{}_3$] (0.19 g, 68%), which was recrystallised from CH_2Cl_2–pentane to give red needles.

Method B. A mixture of [Cr(acac)$_3$] (0.20 g, 0.57 mmol) and HL^1 (0.325 g, 1.9 mmol) in ethylene glycol (30 cm^3) was heated to 175 °C for 3 h whilst bubbling N_2 slowly through the mixture (as for **1**, above). Work-up as for **1** followed by chromatography on alumina (Brockmann activity III) with CH_2Cl_2 gave two products. The first red-brown band to elute was [CrL$^1{}_2$(acac)] **5**, of which 0.072 g (26%) was isolated. This was followed by [CrL$^1{}_3$] **4**, of which 0.151 g (47%) was isolated.

[CrL$^2{}_2$][PF$_6$] **6**. A mixture of [Cr(acac)$_3$] (0.185 g, 0.53 mmol) and HL^2 (0.273 g, 1.1 mmol) in ethylene glycol (20 cm^3) was heated to 175 °C for 3 h with N_2 bubbling gently through the solution. After cooling to room temperature, aqueous NH_4PF_6 was added and the resulting brown precipitate collected by filtration, dried, and purified by chromatography on alumina (Brockmann activity III) with CH_2Cl_2. The major orange band was collected to give pure **6** (0.292 g, 80%), which was recrystallised from acetonitrile–diethyl ether to give red needles.

Crystal-structure Determinations of Compounds **4** *and* **6**.—Data were collected using a Siemens R3m/V four-circle diffractometer (293 K, Mo-Kα X-radiation, graphite monochromator, $\bar{\lambda}$ = 0.710 73 Å). The data were corrected for Lorentz, polarisation and X-ray absorption effects. The structures were solved by conventional heavy-atom or direct methods, and successive Fourier difference syntheses were used to locate all non-hydrogen atoms. All calculations were performed on a DEC micro-Vax II computer with the SHELXTL PLUS system of programs.[12] Scattering factors with corrections for anomalous dispersion were taken from ref. 13.

Additional material available from the Cambridge Crystallographic Data Centre comprises H-atom coordinates, thermal parameters and remaining bond lengths and angles.

[CrL$^1{}_3$]·CH_2Cl_2·0.5C_5H_{12} **4**. Red needle crystals were grown from CH_2Cl_2–pentane and that used had dimensions *ca.* 0.50 × 0.25 × 0.20 mm. To inhibit loss of solvent the crystal was sealed in a capillary tube under nitrogen saturated with CH_2Cl_2–pentane. Of the 3185 data collected (Wyckoff ω scans, $2\theta \leqslant 50°$), 2454 unique data had $F \geqslant 3\sigma(F)$, and only these were used for structure solution and refinement. Resolution of the intensities along the *b* axis [36.943(12) Å] was satisfactory because of the extensive systematic absences associated with the space group *Fdd*2. An empirical absorption correction was applied using a method based upon azimuthal scan data.

Crystal data. $C_{33}H_{18}CrN_3O_3 \cdot CH_2Cl_2 \cdot 0.5C_5H_{12}$, M = 677.5, orthorhombic, space group *Fdd*2, a = 28.130(11), b = 36.943(12), c = 12.894(5) Å, U = 13 400(8) Å^3, Z = 16, D_c = 1.34 g cm^{-3}, F(000) = 5568, μ(Mo-Kα) = 5.4 cm^{-1}.

Crystals of **4** diffracted poorly and insufficient data were observed to allow a full anisotropic refinement. Only the Cr, N and O atoms of the complex and the atoms of the solvent molecules were refined with anisotropic thermal parameters. Hydrogen atoms were included in calculated positions (C–H 0.96 Å) with fixed isotropic thermal parameters (U_{iso} = 0.08 Å^2). The asymmetric unit contains half a molecule of pentane which is disordered about a two-fold axis and a molecule of CH_2Cl_2 which lies in a general position. A Rogers refinement[12] was used to confirm the absolute configuration. Final R = 0.065 (R' = 0.067) with a weighting scheme $w^{-1} = [\sigma^2(F) + 0.001F^2]$. The final electron density difference synthesis showed no peaks > 0.42 or < −0.35 e Å^{-3}.

[CrL$^2{}_2$][PF$_6$]·0.5Et_2O **6**. Red needle crystals were grown from acetonitrile–diethyl ether and that used had dimensions *ca.* 0.20 × 0.20 × 0.60 mm. To inhibit loss of solvent the crystal was sealed in a capillary tube under nitrogen saturated with acetonitrile–diethyl ether. Of the 3613 data collected (Wyckoff ω scan, $2\theta \leqslant 40°$), 1549 unique data had $F \geqslant 3\sigma(F)$, and only these were used for structure solution and refinement. An empirical absorption correction was applied using a method based upon azimuthal scan data.

Crystal data. $C_{32}H_{22}CrF_6N_4O_2P \cdot 0.5Et_2O$, M = 726.6, monoclinic, space group $P2_1/n$, a = 18.833(5), b = 7.935(2), c = 22.727(8) Å, β = 96.01(2)°, U = 3377(2) Å^3, Z = 4, D_c = 1.43 g cm^{-3}, F(000) = 1484, μ(Mo-Kα) = 4.57 cm^{-1}.

Crystals of **6** diffracted poorly and insufficient data were observed to allow a full anisotropic refinement. Only the Cr, N and O atoms of the cation and the atoms of the anion and the solvent molecule were refined with anisotropic thermal parameters. Hydrogen atoms were included in calculated positions (C–H 0.96 Å) with fixed isotropic thermal parameters (U_{iso} = 0.08 Å^2). The asymmetric unit contains half a molecule of Et_2O which is severely disordered across an inversion centre. Because of the nature of the disorder it is not possible to identify a unique location for the oxygen atom and the electron density in this region was most adequately modelled by three carbon atoms with a total site occupation of 2.5. Attempts at modelling the disordered solvent molecule with more than three component atoms led to unstable refinement. Final R = 0.093 (R' = 0.082) with a weighting scheme $w^{-1} = [\sigma^2(F) + 0.0009F^2]$. The final electron density difference synthesis showed no peaks > 0.46 or < −0.35 e Å^{-3}.

Results and Discussion

Syntheses of Complexes.—We had previously attempted to prepare [RuL$^1{}_3$] **1** by reaction of commercial ruthenium trichloride hydrate with three equivalents of the ligand HL^1.[5] We found this to be unsatisfactory, as it led to mixtures of products from which the desired complex could be isolated only with difficulty and in low yield. By contrast the ligand exchange reaction between [Ru(acac)$_3$] and three equivalents of HL^1 at 175 °C works well, as the liberated acetylacetone is volatile and therefore immediately removed from the reaction mixture by the stream of nitrogen bubbles; this is based on a published method for preparation of other tris(chelate) complexes of ruthenium(III).[8] Complex **1** was obtained in 90% yield by this route. The minor product [RuL$^1{}_2$(acac)] **2** was also formed in 9% yield, and the two could be readily separated chromatographically. The complex [Ru(bipy)L$^1{}_2$][PF$_6$] **3** was prepared in a similar manner, by reaction of two equivalents of HL^1 with [Ru(bipy)(acac)$_2$]$^+$ {generated *in situ* from [Ru(bipy)Cl$_3$] and excess of Hacac[14]} at a temperature such that the liberated Hacac immediately evaporates from the reaction mixture.

The complex [CrL$^1{}_3$] **4** could be prepared in one of two ways. Reaction of $CrCl_3 \cdot 6H_2O$ with three equivalents of HL^1 in the presence of Na_2CO_3 in ethanol at reflux gave a 68% yield of **4** after chromatographic purification; alternatively, it could be prepared in a ligand-exchange reaction similar to that used for preparation of [RuL$^1{}_3$], by reaction of [Cr(acac)$_3$] with three

equivalents of HL^1 at 175 °C in ethylene glycol. This method only gave a 47% yield of **4**, but also gave $[CrL^1{}_2(acac)]$ **5** in 26% yield. Finally, $[CrL^2{}_2][PF_6]$ **6** was prepared in good yield from $[Cr(acac)_3]$ by the ligand-exchange method, followed by treatment with KPF_6.

The identities of all of the complexes were confirmed by FAB mass spectrometry and elemental analyses (Table 1). In some of the mass spectra it is noteworthy that, in addition to the expected molecular ion peak, the spectra show additional weak peaks at higher mass corresponding to the presence of two complex units held together either by protons or sodium ions. We have observed behaviour similar to this before, with the complex $[NiL^2{}_2]\cdot 2HPF_6$,[2] in which two pseudo-octahedral $NiL^2{}_2$ units are held in close association by intermolecular hydrogen-bonding between phenolate oxygen atoms. Such behaviour is clearly occurring in these new complexes, and suggests that formation of polynuclear adducts between complexes with an oxygen-rich co-ordination sphere and oxophilic cations may be possible.

Electrochemical Properties.—All three ruthenium complexes **1**–**3** show reversible Ru^{III}–Ru^{IV} oxidations and Ru^{III}–Ru^{II} reductions in acetonitrile [Fig. 1(*a*) and Table 2]; in every case the cathodic and anodic peak currents are equal, and the separation between them is 60–70 mV and independent of scan rate. Complex **1** has an N_3O_3 donor set and **3** has an N_4O_2 donor set, where N denotes a pyridyl ligand and O denotes a phenolate ligand. As expected, replacement of a π-acidic pyridyl ligand by a σ-donating phenolate results in stabilisation of higher oxidation states; both redox couples in **1** are shifted cathodically with respect to those of **3**, by 0.46 and 0.68 V for the +3/+4 and +2/+3 couples respectively. This type of

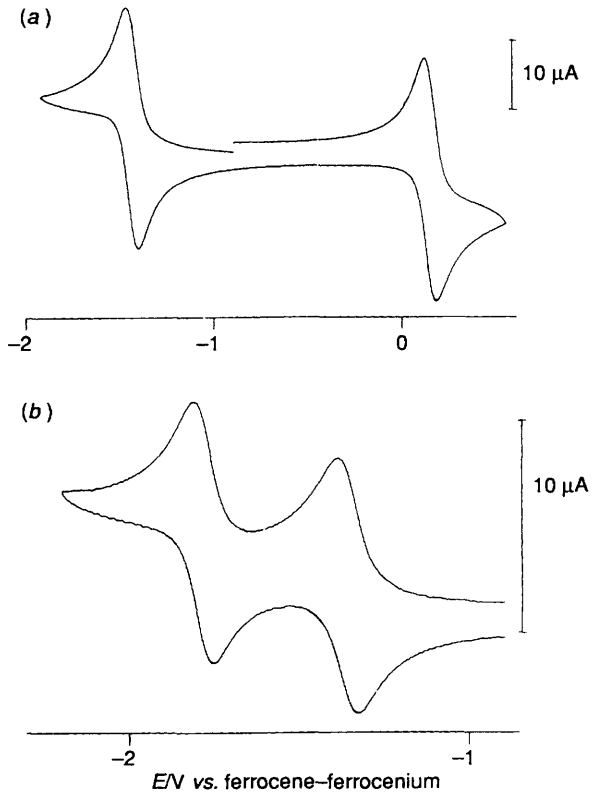

Fig. 1 Cyclic voltammograms of **1** in MeCN at 0.2 V s^{-1} (*a*) (the voltammograms of **2** and **3** are similar), and **6** in MeCN at 0.2 V s^{-1} (*b*)

Table 1 Analytical and spectroscopic data for the new complexes

Complex	Analysis (%) C	H	N	FAB mass spectrum *m/z* [relative intensity (%), assignment]	UV/VIS spectrum λ_{max}/nm (10^{-3} ε/dm^3 mol^{-1} cm^{-1})
1	64.0 (64.8)	3.9 (3.9)	6.9 (6.9)	442 (67, $[RuL^1{}_2]^+$), 612 (100, $[RuL^1{}_3]^+$), 635 (3, $[RuL^1{}_3 + Na]^+$), 884 (< 1, $[(RuL_2)_2]^+$), 1052 (< 1, $[RuL^1{}_2RuL^1{}_3]^+$)	338 (12), 400 (4.7), 541 (2.1), 1524 (0.11),[b] 2150 (0.10)[b]
2	59.9 (60.0)	4.4 (4.3)	5.1 (5.2)	442 (50, $[RuL^1{}_2]^+$), 541 (100, $[RuL^1{}_2(acac)]^+$), 1082 (1, $[\{RuL^1{}_2(acac)\}_2]$), 1105 (< 1, $[\{RuL^1{}_2(acac)\}_2 + Na]^+$)	336 (13), 424 (sh), 540 (2.9), 1500 (0.07),[b] 2080 (0.13)[b]
3·0.5MeCN[c]	51.6 (51.9)	3.5 (3.3)	8.2 (8.3)	442 (18, $[RuL^1{}_2]^+$), 598 (100, $[RuL^1{}_2(bipy)]^+$)	333 (18), 668 (5.1)
4·CH_2Cl_2[d]	63.2 (63.1)	4.4 (4.0)	6.2 (6.5)	222 (22, $[CrL^1]^+$), 392 (100, $[CrL^1{}_2]^+$), 562 (34, $[CrL^1{}_3]^+$), 585 (4, $[CrL^1{}_3 + Na]^+$), 1125 (1, $[\{CrL^1{}_3\}_2 + H]^+$), 1147 (1, $[\{CrL^1{}_3\}_2 + Na]^+$)	380 (12), 559 (0.12)
5	65.8 (66.0)	4.7 (4.7)	5.7 (5.7)	222 (41, $[CrL^1]^+$), 321 (100, $[CrL^1(acac)]^+$), 392 (80, $[CrL^1{}_2]^+$), 491 (74, $[CrL^1{}_2(acac)]^+$), 514 (4, $[CrL^1{}_2(acac) + Na]^+$), 983 (2, $[\{CrL^1{}_2(acac)\}_2 + H]^+$), 1005 (1, $[\{CrL^1{}_2(acac)\}_2 + Na]^+$)	319 (22), 383 (14), 545 (0.17)
6·MeCN[c]	55.7 (55.7)	3.5 (3.4)	9.3 (9.6)	299 (42, $[CrL^2]^+$), 546 (100, $[CrL^2{}_2]^+$), 1092 (7, $[\{CrL^2{}_2\}_2]^+$)	320 (23), 340 (22), 450 (sh)

[a] Calculated values in parentheses. [b] Near-IR peaks recorded in CCl_4. [c] Recrystallised from MeCN–diethyl ether. [d] Recrystallised from CH_2Cl_2–pentane.

Table 2 Electrochemical and EPR data for the new complexes

Complex	Metal redox potentials (V *vs.* ferrocene–ferrocenium)[a] M^{IV}–M^{III}	M^{III}–M^{II}	M^{II}–M^{I}	EPR data g_x	g_y	g_z
1	+0.14 (70)	−1.39 (70)		−2.35	−2.16	−1.85
2	+0.22 (70)	−1.37 (70)		−2.34	−2.12	−1.88
3[b]	+0.60 (70)	−0.71 (70)		−2.53	−2.03	−1.85 [set (*a*)]
				−2.31	−2.12	−1.92 [set (*b*)]
4		−2.26 (80)				
5		−2.28 (100)				
6		−1.37 (70)	−1.79 (60)			

[a] Electrochemical measurements recorded at a Pt-bead working electrode in MeCN with a scan rate of 0.2 V s^{-1}; values in parentheses are peak-peak separations in mV. [b] Mixture of two isomers; see text.

electrochemical behaviour is similar to that observed for tris(chelate)ruthenium(III) complexes of substituted salicylaldimines and derivatives of 8-hydroxyquinoline.[7] Together with the results for $[Ru(bipy)_3]^{2+}$, $[Ru(bipy)_2L^1]^+$ and $[RuL^2_2]^+$ from ref. 5, we now have electrochemical data on a complete series of ruthenium complexes with N_6, N_5O, N_4O_2 (2 examples) and N_3O_3 donor sets which are presented graphically in Fig. 2. There is an excellent linear relationship between ligand set and redox potential for the Ru^{II}–Ru^{III} couples; the best-fit straight line (correlation coefficient > 0.99) has a slope of 0.75 V decrease in the Ru^{II}–Ru^{III} potential per phenolate ligand.

The reductive cyclic voltammograms of the chromium(III) complexes **4**–**6** are summarised in Table 2. Complex **4**, with an N_3O_3 donor set, shows a single reversible one-electron reduction at $E_{\frac{1}{2}} = -2.26$ V *vs.* ferrocene–ferrocenium, which we assign to a metal-based Cr^{III}–Cr^{II} reduction; complex **6**, with an N_4O_2 donor set, undergoes two reversible reductions at more anodic potentials [Fig. 1(*b*)]. Chromium complexes are known to exhibit several oxidation states; for example, $[Cr(bipy)_3]^{3+}$ undergoes reversible +3/+2, +2/+1 and +1/0 reductions, at $E_{\frac{1}{2}} = -0.57$ V, −1.09 V and −1.65 V *vs.* ferrocene–ferrocenium respectively in acetonitrile.[15] The N_4O_2 donor set in **6** results in stabilisation of the +3 oxidation level over +2 by 0.80 V, and of the +2 oxidation level over +1 by 0.70 V with respect to $[Cr(bipy)_3]^{2+}$. Moving a step further to an N_3O_3 donor set results in a further cathodic shift of the +3/+2 couple by 0.89 V (so the variation of redox potential with donor set is clearly not linear here), and the +2/+1 couple is no longer accessible. All three complexes show totally irreversible oxidations at high positive potentials which are probably ligand-based.

Electronic Spectral Properties.—The electronic spectra of **1**–**6** are summarised in Table 1. The ruthenium(III) complexes **1**–**3** all show a moderately intense transition in the visible region which, by analogy with the spectra of similar complexes,[6] are from phenolate-to-ruthenium(III) charge transfer. The intense transition between 330 and 340 nm is undoubtedly an intra-ligand $\pi \longrightarrow \pi^*$ transition in each case. Complexes **1** and **2** both show an additional transition at around 400 nm whose nature is uncertain.

It has been shown that both tetragonal and rhombic distortions from ideal octahedral symmetry in complexes of ruthenium(III) results in a splitting of the (formally) t_{2g} orbital set.[7] If the distortion is sufficiently large, the separations between the three orbitals are such that two transitions between them, resulting in low-lying excited doublet states, may be observed in the near-IR region of the spectrum. In our case the asymmetric nature of the ligand donor sets is sufficient to cause this, and the electronic spectra of **1** and **2** in CCl_4 solution in the near-IR region both clearly show the expected two transitions at around 1500 and 2100 nm, with absorption coefficients of 70–130 $dm^3\ mol^{-1}\ cm^{-1}$. These observations are in excellent agreement with those of ref. 7. Complex **3** is insoluble in CCl_4.

The chromium(III) complexes **4** and **5** both show a weak metal-centred ($^4A_{2g} \longrightarrow {}^4T_{2g}$) transition in the visible region and intense intraligand $\pi \longrightarrow \pi^*$ transitions in the UV region. For **6**, there is an additional shoulder at about 450 nm which is very broad and extends to about 600 nm in the visible region, thereby masking the expected d–d transition. The intensity of this shoulder (approximately 5000 $dm^3\ mol^{-1}\ cm^{-1}$) suggests that it may be a phenolate-to-chromium(III) charge transfer.

EPR Properties.—The EPR spectra at 77 K of **1**, **2** and **3** are shown in Fig. 3; the *g* values are listed in Table 2. Complexes **1** and **2** have typical rhombic spectra with three well resolved components. This means that **1** has a meridional rather than a facial structure; a facial N_3O_3 co-ordination geometry would have C_3 symmetry with *x* and *y* degenerate and therefore result in only two EPR signals, as happens for example in $[Ru(bipy)_3]^{3+}$ which has a three-fold symmetry axis (point group D_3).[16] The sterically favourable meridional geometry by contrast has no symmetry elements (C_1), and is known to occur for $[CoL^1_3]$,[17] $[CrL^1_3]$ (see below), and a variety of other tris(salicylaldimine) complexes of cobalt(III)[18] and ruthenium(III).[7] The spectrum of **2** is similar, consistent with either of the possible isomeric structures; the *cis* isomer would have C_1 symmetry and the *trans* isomer C_2.

The signs of the *g* values may be assigned by comparison with the tris(salicylaldimine)ruthenium(III) complexes of ref. 7. Whilst g_x and g_y are unambiguously negative, g_z may be of

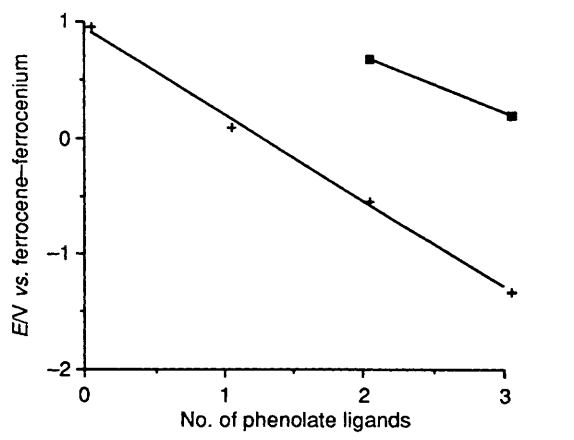

Fig. 2 Variation of Ru^{II}–Ru^{III} (+) and Ru^{III}–Ru^{IV} (■) redox potentials with donor sets varying from N_6 to N_3O_3 (N = pyridyl; O = phenolate). The $E_{\frac{1}{2}}$ values for the N_4O_2 donor set are the average of the values for **3** (this work) and $[RuL^2_2][PF_6]$[5]

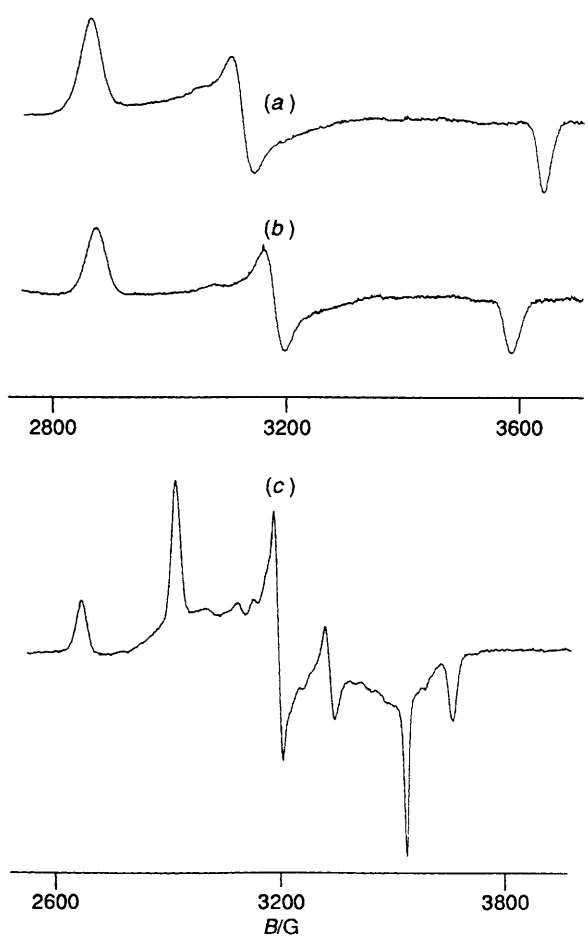

Fig. 3 EPR spectra of **1** (*a*), **2** (*b*) and **3** (*c*) recorded at 77 K in CH_2Cl_2–thf glasses. For **1** and **2**, ν = 9.44 GHz; for **3**, ν = 9.46 GHz

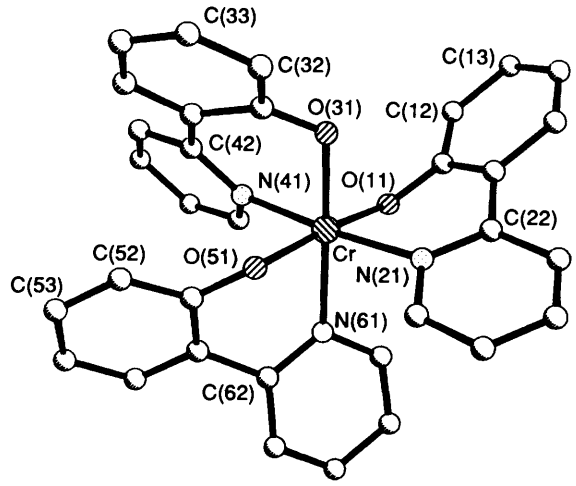

Fig. 4 Structure of $[CrL^1_3]$ **4**

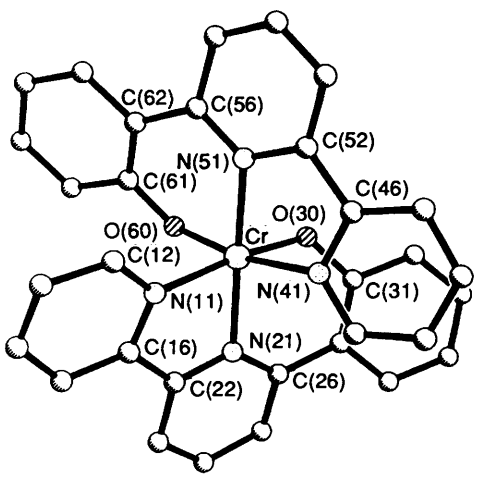

Fig. 5 Structure of the cation $[CrL^2_2]^+$ **6**

Table 3 Selected internuclear distances (Å) and angles (°) for $[CrL^1_3]$ **4**

Cr–O(11)	1.922(6)	O(11)–Cr–N(21)	86.5(3)
Cr–N(2)	2.076(7)	O(11)–Cr–N(41)	89.8(3)
Cr–O(31)	1.922(5)	O(11)–Cr–O(51)	174.4(2)
Cr–N(41)	2.055(6)	N(41)–Cr–O(51)	90.3(2)
Cr–O(51)	1.957(6)	O(31)–Cr–N(61)	176.3(2)
Cr–N(61)	2.122(6)		
O(11)–Cr–O(31)	93.8(3)	N(21)–Cr–O(31)	90.3(2)
N(21)–Cr–N(41)	175.0(3)	O(31)–Cr–N(41)	86.6(2)
N(21)–Cr–O(51)	93.6(3)	O(31)–Cr–O(51)	91.8(2)
O(11)–Cr–N(61)	89.6(3)	N(21)–Cr–N(61)	88.6(2)
N(41)–Cr–N(61)	94.8(2)	O(51)–Cr–N(61)	84.8(2)

either sign if no constraint is placed on the energies of the near-IR transitions. For g_z to be positive requires the presence of two transitions between 6000 and 7000 nm (*i.e.* in the middle of the IR region); for g_z to be negative requires the presence of two transitions between about 1400 and 2200 nm. All three g values are therefore negative.

The spectrum of **3** is more complex than would be expected, with six peaks rather than three. The only explanation for this is that **3** is a mixture of *cis* and *trans* isomers. If the donor atoms are considered to occupy idealised octahedral geometries and the chelate linkages are ignored, the *cis* N_4O_2 isomer has C_{2v} symmetry and the *trans* isomer D_{4h}. The former would give a rhombic spectrum with three separate EPR signals, whereas the latter would give a tetragonal spectrum since x and y would be degenerate. However the presence of the chelate links means that both isomers actually have C_2 symmetry, so both would exhibit rhombic spectra. Integration of the signals clearly shows

Table 4 Atomic positional parameters ($\times 10^4$) for $[CrL^1_3]\cdot CH_2Cl_2\cdot 0.5C_5H_{12}$ **4** with estimated standard deviations (e.s.d.s) in parentheses

Atom	x	y	z
Cr	−5 970(1)	−6 983(1)	10 000
O(11)	−6 137(2)	−7 057(2)	8 570(5)
C(11)	−5 875(3)	−6 925(2)	7 818(7)
C(12)	−6 091(4)	−6 746(3)	6 992(8)
C(13)	−5 817(4)	−6 601(3)	6 171(10)
C(14)	−5 349(4)	−6 637(3)	6 186(10)
C(15)	−5 113(4)	−6 804(3)	6 972(9)
C(16)	−5 374(3)	−6 959(2)	7 812(7)
N(21)	−5 296(2)	−7 165(2)	9 601(6)
C(22)	−5 106(3)	−7 148(2)	8 632(7)
C(23)	−4 665(3)	−7 306(3)	8 430(9)
C(24)	−4 416(4)	−7 464(3)	9 215(8)
C(25)	−4 587(3)	−7 478(3)	10 203(8)
C(26)	−5 041(3)	−7 325(2)	10 357(7)
O(31)	−5 772(2)	−6 491(1)	9 785(5)
C(31)	−5 855(3)	−6 261(2)	10 545(6)
C(32)	−5 486(3)	−6 028(2)	10 880(7)
C(33)	−5 563(4)	−5 777(3)	11 651(8)
C(34)	−5 990(4)	−5 746(3)	12 101(8)
C(35)	−6 356(3)	−5 970(2)	11 828(7)
C(36)	−6 301(3)	−6 230(2)	11 051(6)
N(41)	−6 637(2)	−6 778(2)	10 279(5)
C(42)	−6 705(3)	−6 451(2)	10 740(7)
C(43)	−7 168(3)	−6 332(3)	10 944(8)
C(44)	−7 562(4)	−6 543(3)	10 644(9)
C(45)	−7 478(3)	−6 878(3)	10 167(8)
C(46)	−7 019(3)	−6 977(2)	9 993(8)
O(51)	−5 821(2)	−6 957(1)	11 480(4)
C(51)	−6 153(3)	−7 037(2)	12 164(6)
C(52)	−6 250(3)	−6 812(2)	12 993(7)
C(53)	−6 596(3)	−6 894(3)	13 708(8)
C(54)	−6 862(3)	−7 213(3)	13 616(8)
C(55)	−6 767(3)	−7 450(2)	12 799(7)
C(56)	−6 409(3)	−7 371(2)	12 076(6)
N(61)	−6 161(2)	−7 527(2)	10 327(5)
C(62)	−6 290(3)	−7 645(2)	11 288(6)
C(63)	−6 314(3)	−8 009(2)	11 515(7)
C(64)	−6 218(3)	−8 262(2)	10 780(7)
C(65)	−6 098(3)	−8 153(3)	9 790(8)
C(66)	−6 076(3)	−7 783(3)	9 610(8)
C	2 403(5)	862(4)	5 267(18)
Cl(2)	2 355(2)	1 242(1)	6 020(4)
Cl(1)	1 884(2)	793(2)	4 565(4)
C(1)	1 992(11)	−2 118(12)	2 462(22)
C(2)	2 251(30)	−2 342(15)	1 672(29)
C(3)	2 500	−2 500	2 344(61)

Table 5 Selected internuclear distances (Å) and angles (°) for $[CrL^2_2][PF_6]$ **6**

Cr–N(11)	2.039(12)	N(11)–Cr–N(21)	79.7(5)
Cr–N(21)	2.054(12)	N(11)–Cr–N(41)	97.1(5)
Cr–O(30)	1.895(10)	N(11)–Cr–N(51)	96.6(5)
Cr–N(41)	2.045(13)	N(41)–Cr–N(51)	79.2(5)
Cr–N(51)	2.068(11)	O(30)–Cr–O(60)	89.8(4)
Cr–O(60)	1.882(10)		
N(11)–Cr–O(30)	171.0(5)	N(21)–Cr–O(30)	91.6(5)
N(21)–Cr–N(41)	96.2(5)	O(30)–Cr–N(41)	86.1(4)
N(21)–Cr–N(51)	173.8(5)	O(30)–Cr–N(51)	92.2(4)
N(11)–Cr–O(60)	88.4(4)	N(21)–Cr–O(60)	93.5(5)
N(41)–Cr–O(60)	169.6(5)	N(51)–Cr–O(60)	91.4(4)

Table 6 Atomic positional parameters ($\times 10^4$) for $[CrL^2_2][PF_6]\cdot 0.5Et_2O$ **6** with e.s.d.s in parentheses

Atom	x	y	z
Cr	4424(1)	1238(3)	2286(1)
N(11)	4836(7)	3447(15)	2631(5)
C(12)	4515(9)	4931(24)	2692(6)
C(13)	4788(8)	6297(22)	3038(6)
C(14)	5448(9)	6005(23)	3340(7)
C(15)	5816(9)	4544(22)	3278(7)
C(16)	5499(10)	3276(21)	2916(7)
N(21)	5483(6)	594(17)	2451(5)
C(22)	5844(11)	1682(24)	2811(8)
C(23)	6539(10)	1297(27)	3054(8)
C(24)	6807(10)	−236(24)	2902(7)
C(25)	6438(9)	−1359(25)	2526(7)
C(26)	5737(9)	−882(24)	2274(7)
O(30)	4180(5)	−966(12)	2015(4)
C(31)	4608(6)	−1909(12)	1709(4)
C(32)	5348	−1987	1841
C(33)	5750	−3066	1523
C(34)	5413	−4068	1073
C(35)	4673	−3990	941
C(36)	4271	−2911	1259
N(41)	4456(7)	1840(15)	1414(6)
C(42)	5015(9)	1758(18)	1103(7)
C(43)	4956(9)	1722(18)	503(7)
C(44)	4296(9)	1779(19)	201(8)
C(45)	3699(9)	1939(20)	496(7)
C(46)	3808(10)	2008(19)	1101(7)
N(51)	3395(6)	2105(13)	2068(5)
C(52)	3223(9)	2196(19)	1480(8)
C(53)	2520(10)	2590(21)	1248(8)
C(54)	2047(10)	2758(22)	1661(8)
C(55)	2216(8)	2663(18)	2238(7)
C(56)	2931(9)	2304(19)	2485(7)
O(60)	4216(5)	631(12)	3050(4)
C(61)	3757(6)	1497(13)	3347(5)
C(62)	3139	2298	3095
C(63)	2680	3069	3456
C(64)	2838	3039	4070
C(65)	3456	2238	4322
C(66)	3916	1467	3960
P	7206(3)	1166(11)	941(3)
F(1)	6840(7)	2619(21)	1209(8)
F(2)	7558(6)	717(21)	1567(5)
F(3)	7574(7)	−402(23)	679(8)
F(4)	6863(7)	1589(23)	323(6)
F(5)	6545(6)	56(17)	1011(5)
F(6)	7873(7)	2214(22)	874(7)
C(3)	−253(37)	−724(77)	119(35)
C(2)	794(24)	2373(79)	−2(25)
C(1)	1422(101)	3255(152)	−101(49)

that they split into two sets of three, of approximate relative intensity 1:2 [sets (a) and (b), Table 2]. The EPR spectrum of $[RuL^2_2]^+$, which has a *cis*-N_4O_2 donor set, has two resolved signals at $g = 2.16$ (an inflexion) and 1.92 (negative-going); the expected third signal (g_z) is only apparent as a shoulder on the $g = 2.16$ signal.[5] These are much more similar to set (b) than set (a) in the spectrum of **3**, and we therefore assign the signals of set (b) to the *cis* isomer of **3** and those of set (a) to the *trans* isomer.

The mixture of isomers of **3** behaves as a single compound chromatographically under various conditions (alumina, MeCN–PhMe; silica, CH_2Cl_2–MeOH). Crystallisation from MeCN–Et_2O gave tiny, block-like crystals which were too small to be separated manually and examined. It is interesting that despite the mixture of isomers the cyclic voltammogram is consistent with the presence of a single material; the isomers must be electrochemically equivalent. It is perhaps surprising that a mixture of isomers could occur under the reaction conditions used (ethylene glycol at 175 °C), especially as only single isomers were observed for **1** and **2**.

No EPR spectra could be observed for the chromium complexes **4**–**6** either at room temperature or 77 K.

Structural Studies.—The crystal structures of **4** and **6** have been determined; they are shown in Figs. 4 and 5 respectively. Bond lengths and angles are in Tables 3 and 5, and atomic coordinates are in Tables 4 and 6 respectively. Both complexes have the expected pseudo-octahedral geometries.

The tris(chelate) **4** has a meridional N_3O_3 co-ordination geometry, in common with both $[CoL^1_3]$[17] and $[RuL^1_3]$ (above). The geometry is slightly distorted from ideality, with the co-ordination-sphere bond angles lying in the range 84.8–94.8°. Co-ordination of the bidentate ligands is accompanied by substantial inter-ring twists. These cannot be defined accurately since the centres of the two rings of each ligand do not necessarily lie on the same line as the inter-ring C–C bond, but approximate inter-ring torsion angles for the three ligands are 24, 26 and 37°. The molecule is chiral and crystallises in the chiral space group *Fdd*2, which means that spontaneous resolution occurs with only one enantiomer present in each crystal.

The geometry of **6** is slightly more distorted, with bond angles at the metal centre lying in the range 79.2–97.1°. The co-ordination-sphere bond lengths are marginally shorter than in **4** (average Cr–O distances are 1.889 Å in **6** and 1.934 Å in **4**; average Cr–N distances are 2.052 Å in **6** and 2.084 Å in **4**) which is probably a consequence of the fact that **6** is cationic whereas **4** is neutral. As usual, the ligands are distorted from planarity, with inter-ring torsion angles of *ca.* 11 (pyridyl–pyridyl) and 25° (pyridyl–phenolate) in one ligand, and 2 and 16° in the other. More unusually, there is a π-stacking interaction between a phenolate ring (ring 3 according to the numbering scheme) of one complex cation and a pyridyl ring (ring 1) of an adjacent complex cation. The average distance of the atoms in ring 1 of one complex to the mean plane of the atoms in ring 3 of its neighbour is 3.71 Å; this interaction possibly explains why the ligand containing rings 1–3 is much more distorted from planarity than the other ligand. The appearance of substantial inter-ring torsion angles to optimise intermolecular π-stacking interactions has been noted before with complexes of L^2.[2]

Acknowledgements

We thank Dr. John Maher for recording the EPR spectra, and the SERC for funds to purchase the EPR spectrometer.

References

1 J. C. Jeffery, E. Schatz and M. D. Ward, *J. Chem. Soc., Dalton Trans.*, 1992, 1921.
2 J. C. Jeffery and M. D. Ward, *J. Chem. Soc., Dalton Trans.*, 1992, 2119.
3 B. M. Holligan, J. C. Jeffery and M. D. Ward, *J. Chem. Soc., Dalton Trans.*, 1992, 3337.
4 J. P. Maher, P. H. Rieger, P. Thornton and M. D. Ward, *J. Chem. Soc., Dalton Trans.*, 1992, 3353.
5 B. M. Holligan, J. C. Jeffery, M. K. Norgett, E. Schatz and M. D. Ward, *J. Chem. Soc., Dalton Trans.*, 1992, 3345.
6 Z. Shirin and K. Mukherjee, *Polyhedron*, 1992, **11**, 2625; K. S. Murray, A. M. van der Bergen and B. O. West, *Aust. J. Chem.*, 1978, **31**, 203; G. S. Rodman and J. K. Nagle, *Inorg. Chim. Acta*, 1985, **105**, 205.
7 G. K. Lahiri, S. Bhattacharya, B. K. Ghosh and A. Chakravorty, *Inorg. Chem.*, 1987, **26**, 4324 and refs. therein.
8 K. S. Finney and G. W. Everett, *Inorg. Chim. Acta*, 1974, **11**, 185.
9 S. Yamada and K. Iwasaki, *Bull. Chem. Soc. Jpn.*, 1968, **41**, 1972; F. Calderazzo, C. Floriani, R. Henzi and F. L'Epplattenier, *J. Chem. Soc. A*, 1969, 1378; J. E. Gray and G. W. Everett, jun., *Inorg. Chem.*, 1971, **10**, 2087; R. Lancashire and T. D. Smith, *J. Chem. Soc., Dalton Trans.*, 1982, 693.
10 S. Anderson and K. R. Seddon, *J. Chem. Res.*, 1979, (*S*) 74 and refs. therein.
11 A. Endo, M. Watanabe, S. Hayashi, K. Shimizu and G. P. Sato, *Bull. Chem. Soc. Jpn.*, 1978, **51**, 800.

12 G. M. Sheldrick, SHELXTL programs for use with a Siemens X-ray System, Cambridge University, 1976; updated Göttingen, 1981.
13 *International Tables for X-Ray Crystallography*, Kynoch Press, Birmingham, 1974, vol. 4.
14 F. P. Dwyer, H. A. Goodwin and E. C. Gyarfas, *Aust. J. Chem.*, 1963, **16**, 42.
15 J. T. Hupp and M. J. Weaver, *Inorg. Chem.*, 1984, **23**, 3639.
16 R. E. DeSimone and R. S. Drago, *J. Am. Chem. Soc.*, 1970, **92**, 2343.
17 P. Ganis, A. Saporito, A. Vitagliano and G. Valle, *Inorg. Chim. Acta*, 1988, **142**, 75.
18 A. Chakravorty and R. H. Holm, *Inorg. Chem.*, 1964, **3**, 1521.

Received 18*th March* 1993; *Paper* 3/01563G